

Are your **MRI contrast agents** cost-effective?

Learn more about generic **Gadolinium-Based Contrast Agents**.



FRESENIUS
KABI

caring for life

AJNR

MR Imaging of Chiari II Malformation

Taher El Gammal, Edward K. Mark and Betty S. Brooks

AJNR Am J Neuroradiol 1987, 8 (6) 1037-1044

<http://www.ajnr.org/content/8/6/1037>

This information is current as
of April 20, 2024.

MR Imaging of Chiari II Malformation

Taher El Gammal¹
Edward K. Mark²
Betty S. Brooks¹

High-field-strength MR imaging was performed in one patient with Chiari III and 19 patients with Chiari II malformations. The MR features were compared with descriptions in the literature and correlated with previously described surgical and postmortem findings and with the results of previous radiologic investigations in this group of patients. Several new observations were apparent from the MR examinations. In 75% of the 20 cases, the underdeveloped tentorium with a wide incisura allowed inferior displacement of the medial posterior cerebrum, which appeared closely applied to a flattened aspect of the superior cerebellum. Previously reported CT descriptions of "pseudotumor of the tentorium" and "towering cerebellum" may be more related to the technique of the radiologic examination than to true upward herniation of the cerebellum. Elongation of the mesencephalon with increase in the mamillopontine distance was present in the majority of our cases and has not been previously emphasized. Some patients had atypical changes or appeared to be borderline cases between the Chiari I and Chiari II categories of malformation, and MR provided considerable diagnostic assistance in these cases.

The noninvasive, in vivo evaluation of MR contributed a great deal to our further understanding of this congenital Chiari malformation.

We report our experience with 19 cases of Chiari II and one of Chiari III malformation examined with high-field-strength MR imaging. Information obtained in the past has relied on autopsy material, surgical observations, and investigative radiologic procedures such as air studies, CT, myelography, and CT myelography. MR provides a new viewpoint with in vivo, detailed anatomic images that can be correlated with the knowledge from previous methods of study of this interesting developmental malformation.

Subjects and Methods

Twenty patients 1 day to 25 years old and including one stillborn infant were evaluated. There were eight males and 12 females. Every patient had hydrocephalus and all had myelomeningocele, except one with an encephalocele at the craniovertebral junction (Chiari III) and diastematomyelia in the lumbar region. All but two had had shunts placed before the MR study. In five, MR was performed at the time of initial diagnosis of Chiari II. In the other 15, MR was performed during follow-up outpatient visits to the Neurosurgery Clinic.

MR examinations were performed with a General Electric 1.5-T Signa system. Limited T1-weighted sagittal series-only studies were performed with a repetition time (TR) of 800 and echo time (TE) of 25 msec, four excitations, 24-cm field of view, and 256 × 256 matrix. For infants younger than 3 months old, a TR of 1000 msec was used. The slice thickness was 3 mm with 1-mm interval interslice spacing in all patients except one, for whom 5-mm-thick slices were used. Three patients also had MR studies of the spine, cervical in two and lumbar in one. In three patients a complete cranial MR study was performed, which included a coronal and transaxial spin-echo pulse sequence series with TR = 2000 msec and TE = 25, 50 or TE = 25, 65 msec. Sedation was given in all cases, most often with IV Seconal at a dose of 2 ml/kg.

This article appears in the November/December 1987 issue of *AJNR* and the January 1988 issue of *AJR*.

Received February 12, 1987; accepted after revision May 4, 1987.

Presented at the annual meeting of the American Society of Neuroradiology, San Diego, January 1987.

¹ Department of Radiology, Section of Neuroradiology, Medical College of Georgia, 1120 15th St., Augusta, GA 30912. Address reprint requests to T. El Gammal.

² Department of Surgery, Section of Neurosurgery, Medical College of Georgia, Augusta, GA 30912.

AJNR 8:1037-1044, November/December 1987
0195-6108/87/0806-1037

© American Society of Neuroradiology

Results

Craniovertebral Junction, Cervical Spinal Canal, and Cervical Cord

Caudal displacement of cerebellar tissue was present in every case. The inferior tip of the vermis was located between the C2–C3 level in the majority of cases. In 10 patients (50%), herniated vermis could be clearly delineated as being separate from the cerebellar tonsils. Tonsillar herniation without evidence of vermian ectopia was noted in one patient.

Medullary herniation with resultant kinking or "spur" at the cervicomedullary junction was found in 15 of 19 patients and could not be evaluated in one patient with a very large head because the image included only the uppermost cervical region.

Hydromyelia was demonstrated by cranial MR in three cases; in one patient cranial and spinal MR failed to reveal a hydromyelia after surgical drainage.

Brainstem, Aqueduct, and Fourth Ventricle

Stretching and inferior displacement of the aqueduct and fourth ventricle was demonstrated in 15 patients. In five of these, the fourth ventricle was significantly dilated with massive dilatation in one. Aqueductal stenosis was found in eight cases.

Elongation and inferior displacement of the brainstem was noted in 15 of 20 patients. The pons appeared flattened in all of these patients. A concave clivus with a wide prepontine subarachnoid space was associated with eight of the 15 (Figs. 1–3). In one, the pons was noted pressing against a straight clivus.

In four other patients a normal brainstem was found. The last case was intermediate between the patients with normal

brainstem and those with definite elongation and caudal displacement (Fig. 4), with mild changes of a slightly stretched aqueduct and fourth ventricle and minimal flattening of the pons.

Relationship of the Tentorium and Superior Surface of the Cerebellum

In 15 of 20 patients MR revealed a definitely flattened appearance of the superior aspect of the cerebellum. The superior surface of the vermis was close to the level of the foramen magnum in three. In four of these 15 patients a notably vertical orientation of the straight sinus was evident, consistent with a wide tentorial incisura (Figs. 1B and 3). The medial posterior cerebrum could be seen in close relation to the flattened superior cerebellum in the majority of these 15 patients.

In two patients with complete cranial MR studies the ventricular trigones were noted to be close together near the midline, again indicative of inferior displacement of the cerebral hemispheres in relation to the tentorium and flattened superior cerebellum.

Mesencephalon, Mamillopontine Distance, and Third Ventricle

In 12 patients, pointing or "beaking" of the quadrigeminal plate consequent to fusion of the colliculi was seen. There was vertical elongation of the mesencephalon with increase in the mamillopontine distance in 10 cases. Measurement of the mamillopontine distance varied between 1.3 and 3.0 cm as a computer-corrected actual patient size measurement. Normal values in adult patients do not exceed 1.2 cm [1]. In

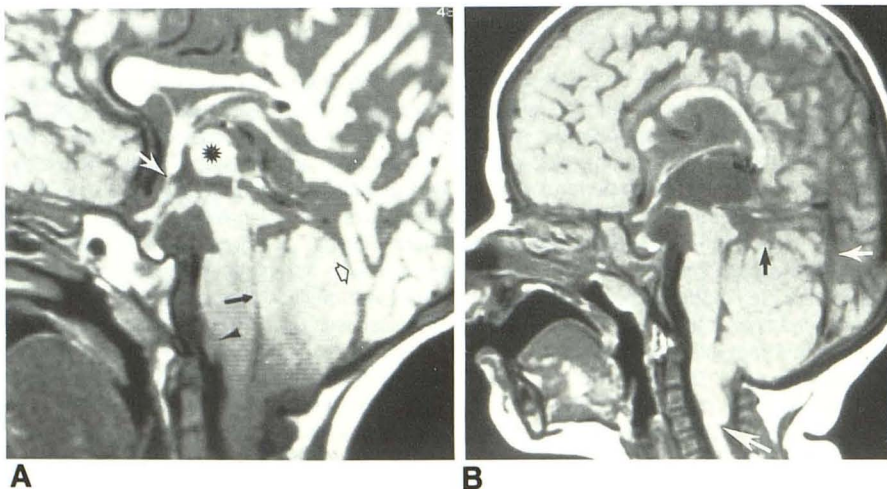


Fig. 1.—Advanced changes of Chiari II malformation in two patients with long-term shunting.

A, Aqueduct and fourth ventricle are stretched (solid black arrow); there is a large massa intermedia (asterisk) and pseudodiverticulum of lamina terminalis (white arrow). Note flattened pons away from concave clivus and pointed quadrigeminal plate. Apparent lobulation of lower pons (black arrowhead) is produced by encircling of brainstem by cerebellar hemisphere. Note increase in mamillopontine distance. Atrophic posterior parietal lobe is herniated through wide tentorium (open arrow), and superior aspect of cerebellum appears flat. Aqueduct is incompletely seen and may be blocked.

B, Stretching of brainstem with elongation of mesencephalon with increase in mamillopontine distance. Again, flat pons is situated at some distance from concave clivus. The massa intermedia is absent, and diverticula are in relation to hypothalamus and lamina terminalis. Defect in anterior corpus callosum is from shunt procedure. There is also a pointed quadrigeminal plate and aqueduct stenosis. Note kink between medulla oblongata and upper cervical cord (large white arrow). Superior surface of vermis is flattened (black arrow) with herniation of medial posterior hemisphere through tentorium. Straight sinus is vertical (small white arrow). Aqueduct is probably obstructed in its midportion.

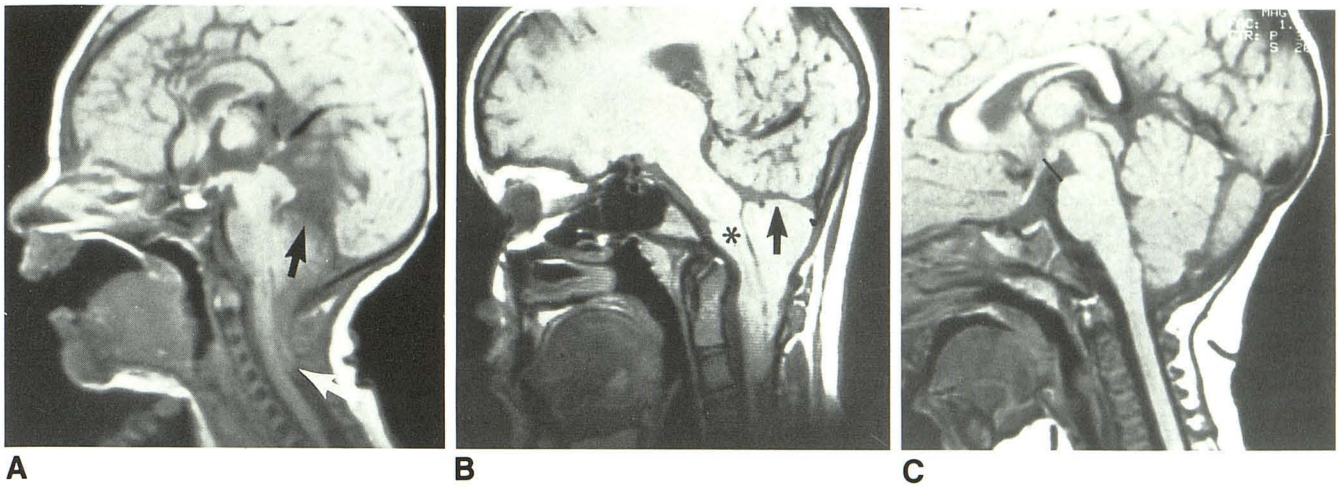


Fig. 2.—A and B, Two patients with severe inferior location of cerebellum.
A, Significant inferior location of cerebellum and flattened superior cerebellum (*black arrow*). Kink between medulla oblongata and spinal cord is indicated (*white arrow*).
B, Severe inferior displacement of cerebellum. Superior cerebellum is flat (*arrow*) and is seen just above foramen magnum with adjacent herniated cerebellum. Pons is flat (*asterisk*), lying just above odontoid. There is severe stretching of mesencephalon with marked increase in mamillopontine distance.
C, Normal study in 8-month-old child shows normal mamillopontine distance (*black line*). Note normal appearance of pointed superior vermis.

Fig. 3.—Chiari II malformation with hydromyelia in 10-year-old girl.

A, Large massa intermedia (*asterisk*), low stretched fourth ventricle (*short black arrow*), hydromyelia (*long black arrow*), and herniated cerebellar vermis (*arrowhead*). There is diverticulum of third ventricle in relation to mamillary body (*short white arrow*). Clivus is concave (*long white arrow*), with considerable distance separating it from flattened pons. Quadrigeminal plate is pointed. Extremely attenuated corpus callosum as well as atrophy of posterior cerebrum resulting in large subarachnoid space above apex of tentorium may be from pressure atrophy from previous hydrocephalus.

B, Note vertical, posteriorly placed straight sinus (*black arrow*) and long vein of Galen (*white arrow*).

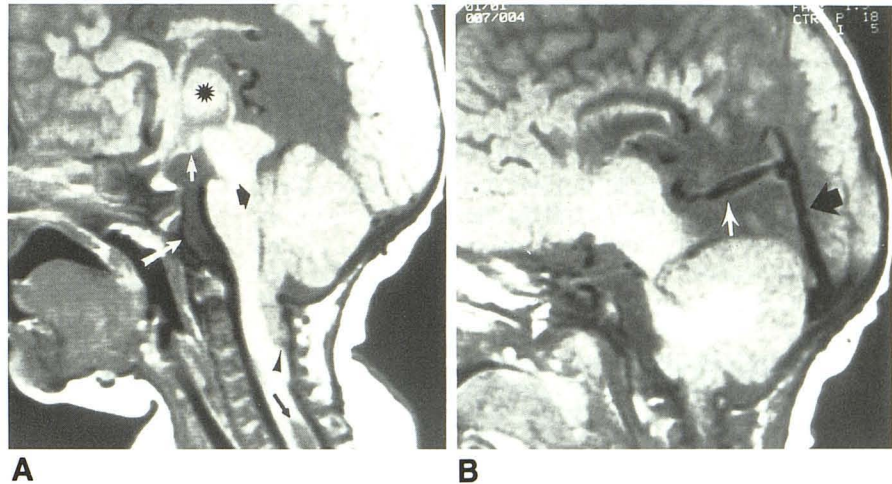
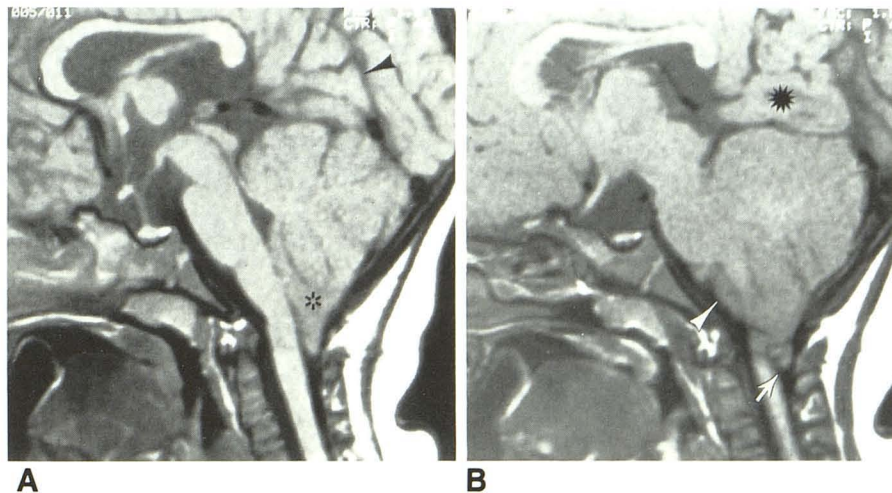


Fig. 4.—1-year-old girl with milder changes of Chiari II malformation. Fourth ventricle and aqueduct are only slightly stretched. Cerebellar ectopia includes both inferior vermis and tonsil (*asterisk*, **A**; *arrow*, **B**). Tentorial opening is wide and there is vertical orientation at line of attachment along straight sinus that was shown in contiguous section (*arrowhead*, **A**). Herniation of medial temporoparietal cerebellum (*asterisk*, **B**) through wide tentorium above flattened superior vermis of cerebellum. Belly of pons appears relatively flattened. In **B**, anterior portion of cerebellum encircles brainstem (*arrowhead*).



two patients, the mamillopontine distance was diminished. The reduction was severe in one of these, in whom there was marked distension of the supratentorial ventricles owing to hydrocephalus. In this patient the mamillary body was seen nearly touching the pons. In the other patient, the brainstem and midline ventricles appeared normal.

Diverticula and pseudodiverticula of the third ventricle were noted in 10 patients. In five, the pseudodiverticula with accessory massa intermedia were seen in relation to the lamina terminalis. In two patients, the diverticula arose from the floor of the hypothalamus, and in three, there were diverticula present in relation to both the hypothalamus and the lamina terminalis.

A large (greater than 1 cm actual patient measurement) massa intermedia was found in 11 patients. An accessory massa intermedia close to but separate from the lamina terminalis was noted in two patients. One of our cases also showed complete obliteration of the third ventricle, most likely as a result of inflammatory changes occurring after chronic shunting.

Discussion

A detailed description of the morbid findings in a full-term infant with spina bifida, craniolacunae, herniation of cerebellar vermis, elongated brainstem, and fourth ventricle through the foramen magnum was first published by Clealand [2] in 1883. In 1891, Chiari [3] reported the morbid findings in infants with varying degrees of hindbrain deformity, and he classified them into three types (I, II, and III). In 1894, Arnold [4] reported one infant with fourth ventricular and cerebellar herniation. Contributions and observations of numerous authors over the years have resulted in the elaboration of many of the neuroanatomic features now regarded as part of the Arnold-Chiari [5-7] or Chiari II [8] malformation.

The radiologic features and evaluations of Chiari II using air studies and polytomography have been reported [8-12], and subsequently water-soluble contrast media have been used to delineate the midline ventricles [13, 14]. Recently, Naidich et al. [15-18] described the CT features of Chiari II with surgical and pathologic correlation.

Currently, high-field-strength MR affords the opportunity for noninvasive evaluation of all the distinctive features of this congenital malformation.

Cervical Spinal Canal and Hydromyelia

Inferior displacement of stretched brainstem with kink between the medulla oblongata and the spinal cord associated with vermian herniation constitute the most important pathologic features of Chiari II malformation [6, 7]. These abnormalities below the foramen magnum have been shown radiologically with oily contrast media [9], by air studies [8, 19], and more recently with water-soluble contrast material in combination with both conventional tomography and CT [18].

With MR, the typical findings of cerebellar vermian herniation and spinomedullary kink or spur in the upper cervical region were found in 15 of 20 patients (Figs. 1, 2A, and 2B) and hydromyelia was demonstrated by cranial MR in three (15%) of 20 cases in our series (Fig. 3). The frequency of hydromyelia in pathologic reports has varied between 20-83% [6, 7] (Table 1). The frequency in our series may be falsely low because sagittal MR in the majority of patients only included the upper cervical spinal canal. Hydromyelia is most frequently demonstrated in the lower cervical and dorsal regions [6] and therefore may have been missed in 17 of our cases. In six of 26 cases reported by Cameron [6], narrowing of the distended central canal in the upper cervical region was found. In two patients who had water-soluble contrast media examinations, this same finding was seen (Figs. 5 and 6). Since the majority of patients (18 of 20) were studied after shunting, collapse of the hydromyelic cavity after shunting may also have contributed to a falsely low frequency in this series. Hall et al. [20] provided some insight into the importance of shunting in Chiari II patients in a report of five cases with severe progressive spasticity. Three patients had definite improvement after shunting of the lateral ventricles. This was postulated to be from collapse of the hydromyelia, which they demonstrated with Pantopaque studies. For the patient in Figure 5, a severe progressive spasticity showed similar, very significant clinical improvement after drainage of the hydromyelia to the cervical subarachnoid space.

Cerebellum and Tentorium

In 35% of a series of cases examined postmortem by Peach [7], upward herniation of the cerebellum was described. Radiologically, Zimmerman et al. [21] reported the CT appear-

TABLE 1: Comparison Between Current MR Findings of Chiari II Malformations and Previous Postmortem Studies

Finding	% of Cases (No.)		
	Present series (n = 20)	Cameron [6] (n = 26)	Peach [7] (n = 20)
Elongation of brainstem and low medulla; stretched aqueduct and fourth ventricle	75 (15/20)	96	90
Kinking of medulla on spinal cord	79 (15/19)	Noted	55
Caudal cerebellum	100 (20/20)	96	90
Hydromyelia	15 (3/20)	83	20
Beaking of quadrigeminal plate	60 (12/20)	Noted	75
Large massa intermedia	55 (11/20)	63	90
Large fourth ventricle	25 (5/20)	Not noted	25

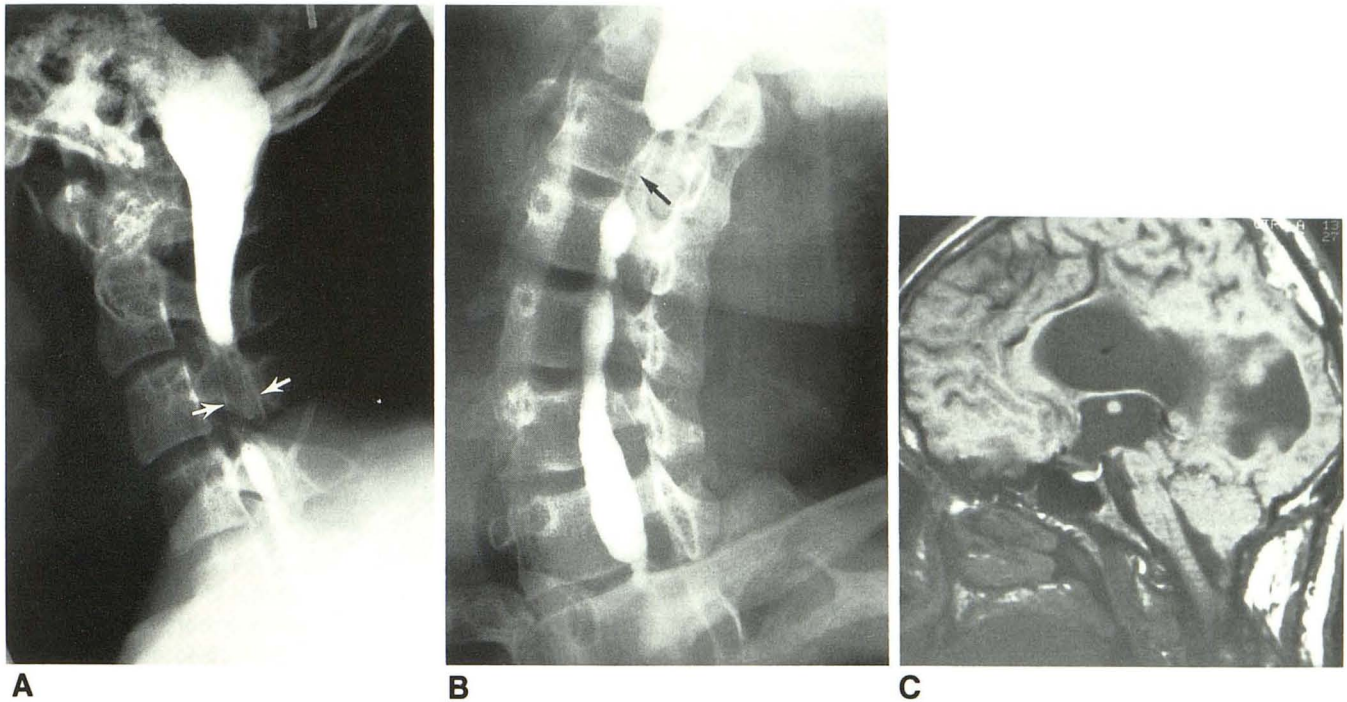


Fig. 5.—17-year-old boy with hydromyelia shown by intraventricular metrizamide.

A and B, Lateral (A) and oblique (B) radiographs after intraventricular metrizamide show hydromyelia with narrowed segment in upper cervical region (arrow, B). Dilated fourth ventricle merges imperceptibly into hydromyelia. Poor filling of hydromyelia behind body of C3 may be from adhesions (arrows, A).

C, Stretching of brainstem and aqueduct, and dilated fourth ventricle. Superior vermis is flat. Mamillopontine distance is increased and pons appears flat. Caudally displaced parietal lobe rests on top of flattened vermis. MR was performed after shunting of syrinx to subarachnoid space, which is why fourth ventricle appears smaller than in A and B.

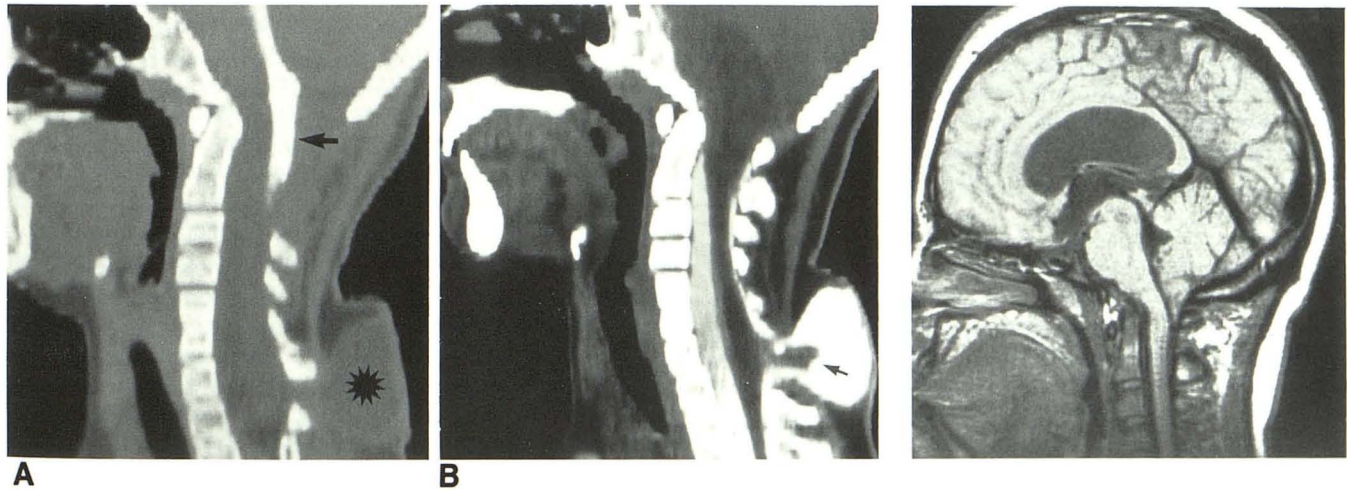


Fig. 6.—Chiari II malformation with stenosis between fourth ventricle and hydromyelia.

A, Sagittal reformatted CT ventriculogram shows low fourth ventricle, which does not appear to communicate with hydromyelia in cervical cord. There is meningocele at cervicothoracic junction (asterisk).

B, Sagittal reformatted CT myelocisternogram shows expanded hydromyelic cord extending into meningocele (arrow). Cerebellar ectopia is evident at craniovertebral junction. Transaxial IV-enhanced CT section just above meningocele (not shown) revealed hydromyelia that did not communicate with fourth ventricle probably because of narrowing of its upper part.

Fig. 7.—Chiari I malformation. Midsagittal MR shows pointed, inferiorly displaced tonsil; angulation between medulla oblongata and cervical spinal cord; expanded trumpeted upper medulla; and rounded belly of the pons. Mamillopontine distance is reduced, partly because of hydrocephalus.

ance of "pseudotumor of the tentorium" in meningomyelocele patients, and Naidich et al. [16] later used the term "towering cerebellum," which was attributed to upward herniation from the inability of the small posterior fossa in Chiari II patients to accommodate posterior fossa contents. However, in 15 (75%) of our 20 cases examined by MR, the intracranial cerebellum appeared small, and the medial posterior cerebrum was clearly seen below the level of the straight sinus adjacent to the midline above the superior aspect of the cerebellar vermis, which had a flat appearance (Figs. 1, 2, 4, and 5C). We noted a fairly normal triangular configuration of the superior cerebellar vermis in three other cases, and in two patients there was an intermediate appearance between the normal and the horizontal or flattened shape seen in the other 15.

In two patients, the intracranial cerebellum did appear large with a high position of the vermis. In both patients, the attachment of the tentorium was normal in position with a normal forward inclination and orientation of the straight sinus. There was elongation and caudal displacement of the fourth ventricle in both. The cerebellar tonsils and inferior vermis were caudally displaced in one patient, and in the other, only the tonsils were positioned below the foramen magnum.

An abnormal vertical orientation of the straight sinus was found in four of our 20 patients, and in three of these the apex of the tentorium was also high (Figs. 1B and 3B). This correlates with the observation made by McCoy et al. [8] that the falcotentorial junction may be located in an unusually high position in the midline, although the underdeveloped tentorial leaflets then extend inferiorly and laterally in an abnormally low position. This results in a very large tentorial incisura. In our three patients in whom transaxial MR was performed, the medial aspects of the posterior cerebral hemispheres were observed close to the midline, and the ventricular trigones appeared to approach one another. In midsagittal and parasagittal sections close to the midline, the medial posterior cerebrum was demonstrated below the falcotentorial junction in apposition to the flattened surface of the cerebellum (Figs. 1, 2B, 4, and 5C). MR observations are consistent with the concept, therefore, that upward herniation of the cerebellum will be seen less often in Chiari II as the severity of the degree of the tentorial hypoplasia increases, and in fact, there is downward displacement of the medial posterior cerebrum adjacent to the midline.

Transaxial CT studies with standard 20° angulation to the canthomeatal plane may produce a "pseudotumor of the tentorium" appearance because inferior posterior fossa sections at the level of the low tentorial hiatus will demonstrate a component of the cerebellum that appears relatively large in comparison with the small amount of the inferiorly located posterior cerebral hemispheres. In normal patients, posterior sections at these levels include only the cerebellum. Coronal sections were not obtained in most of our cases; however, it is expected they would have confirmed our observations in the sagittal projection and may possibly have added other information as well.

A wide subarachnoid cistern above the cerebellum has been noted on CT studies [17]. This may occur consequent to parenchymal loss in the medial posterior aspects of the cerebral hemispheres owing to pressure atrophy from hydro-

cephalus in some patients (Figs. 1A and 3). Peach [7] made pathologic observations of brain-tissue loss involving inferior and posterior portions of the cerebral hemispheres in some of his patients, and this has also been demonstrated radiologically on air studies [10].

Pons and the Concave Clivus

A flattened pons, noted in 15 of our 20 patients, was found to be associated with concavity of the clivus in eight. MR demonstrated that the concavity involved the basioccipital portion while the basisphenoid remained straight (Figs. 1, 3, and 5C), consistent with previous observations by Yu and Deck [22], who suggested that this could be caused by pressure effect of the pons against the clivus. However, polytome air studies in some patients have shown that the pons may be situated a considerable distance from the concave clivus [12, 23]. This observation as well as the MR studies both mitigate against the theory of pressure effect on the clivus by the pons.

Fourth Ventricle and the Aqueduct

In five of 20 cases in this series, dilatation of the inferiorly displaced fourth ventricle was noted. This has been reported from autopsy material [7, 24] and has been shown on air studies [11, 12].

A double-humped appearance of the inferiorly displaced fourth ventricle in Chiari II has also been demonstrated by air studies [8, 9, 11, 12] and attributed to bulging of the inferior vermis [8]. This double-humped appearance was not seen in any of our cases studied with MR.

CT without the use of water-soluble contrast media has not provided adequate delineation of the aqueduct, and this represents a clear-cut advantage of the direct sagittal imaging capability of MR. MR sections 3 mm or less in thickness should be used for consistent and proper delineation of the aqueduct. Nonvisualization is then highly suggestive of aqueduct obstruction. MR may not depict physiologic obstruction, however. Intraventricular contrast studies with air movement from the third ventricle to a low fourth ventricle was noted in apparent aqueduct obstruction [9, 10, 12]. In older children, chronic inflammatory changes after shunting may also result in structural blockage of the aqueduct, contributing to an increased occurrence of aqueduct obstruction with the age of the patient and with shunting.

Mesencephalon and Third Ventricle

Beaking of the quadrigeminal plate, first reported by Cleland [2] in 1883, represents a characteristic morphologic finding in Chiari II patients [6, 7]. Elongation of the mesencephalon, however, has not been stressed in the previous pathologic or radiologic literature and was clearly shown by MR in 50% of the cases in our series. This was confirmed by measurement of the mamillopontine distance, and the values found were well above the normal adult range [1] (Fig. 2C), with measurements of up to 3.0 cm.

TABLE 2: Hindbrain Abnormalities in Chiari I and II Malformations

Feature	Chiari I	Chiari II
Mamillopontine distance	Reduced	Increased
Beaked quadrigeminal plate	No	Yes
Junction between spinal cord and medulla	May show angulation	Kinking or "spur"
Pons	Round	Flat
Medulla oblongata	"Trumpet-shaped" with increased antero-posterior diameter at medullopontine junction	Stretched and low
Cerebellar ectopia	Tonsils	Vermis \pm tonsils

The large massa intermedia is a well-known feature associated with Chiari II [6, 7], and other specific morphologic changes seen in the third ventricle have included accessory massa intermedia, diverticula, and pseudodiverticula [9–12, 25]. The pseudodiverticula caused by accessory massa intermedia close to the lamina terminalis have been seen infrequently by air studies in normal patients [26]. A hypothalamic, slitlike recess of the third ventricle was reported in normal cases [27]. These observations are difficult to make with cranial CT, but are clearly outlined with MR (Figs. 1 and 3).

Intermediate Cases

In all of our cases, myelomeningocele was present. In a 1957 review of the literature, Cameron [6] found no report of a myelomeningocele without an associated Chiari II malformation. His postmortem examination of 26 patients with myelomeningocele included two cases with a normal brain and craniovertebral junction, one patient with features of Chiari I malformation, and one atypical case with slight elongation of the brainstem and fourth ventricle but no cerebellar ectopia. A case of myelomeningocele with normal appearance of the midline ventricles has also been illustrated on air studies [9]. On the other hand, classical anatomic features of Chiari II malformation involving cranium and cervical spinal canal have been reported without a myelomeningocele [28, 29]. There is, therefore, a spectrum of changes in hindbrain malformations and myelomeningoceles. In our series, there were five atypical cases. The brainstem appeared nearly normal in four. In one patient, stretching and inferior displacement of the brainstem and fourth ventricle was present, with tonsillar herniation as the only cerebellar ectopia. Included in our series is a case of Chiari III that also had lumbar diastematomyelia. Diastematomyelia of the cervical cord has been demonstrated with water-soluble contrast studies in Chiari II malformations [18].

The most useful features in the distinction of the Chiari I anomaly, illustrated in Figure 7 (El Gammal T, unpublished data), from the Chiari II malformation are summarized in Table 2. MR reveals the relationship of the soft tissues and osseous structures without the artifacts of postmortem examination. MR now provides, noninvasively and with the proper delineation of brainstem, cerebellum, and spinal canal, the best imaging method in the evaluation of borderline cases.

REFERENCES

1. El Gammal T, Allen MB Jr, Brooks BS, Mark EK. MR evaluation of hydrocephalus. *AJNR* 1987;8:591–597
2. Clealand J. Contribution to study of spina bifida encephalocele and anencephalus. *J Anat* 1883;17:257–291
3. Chiari H. Über Veränderungen des Kleinhirns Infolge von Hydrocephalie des Grosshirns. *Dtsch Med Wochenschr* 1891;17:1172–1175
4. Arnold J. Myelocyste transposition von gewebskeimen and Symbodie. *Beitr Pathol* 1894;16:1–28
5. Schwalbe E, Gredig M. Über entwicklungsstörungen des Kleinhirns, hirns-tamms und halsmarks bei spina bifida. *Beitr Pathol* 1907;40:132–194
6. Cameron AH. The Arnold-Chiari and other neuroanatomical malformations associated with spina bifida. *J Pathol* 1957;73:195–211
7. Peach B. Arnold-Chiari malformation anatomic features of 20 cases. *Arch Neurol* 1965;12:613–621
8. McCoy WT, Simpson DA, Carter RF. Cerebral malformations complicating spina bifida: radiological studies. *Clin Radiol* 1967;18:176–182
9. El Gammal T. Extra-ventricular (communicating) hydrocephalus: some observations on midline ventricles. *AJR* 1969;106:308–328
10. El Gammal T. Follow-up air studies on patients with ventriculoatrial (V-A) shunts reference to the value of polytomography. *AJR* 1973;118:155–162
11. El Gammal T, Allen MB Jr, Lott T. Computer assisted tomography and pneumoencephalography in non-tumorous hydrocephalus in infants and children. *J Comput Assist Tomogr* 1977;1(2):204–210
12. El Gammal T, Allen MB Jr. *An atlas of polytome pneumography*, vol 4. Springfield, IL: Thomas, 1977:175–195
13. Fitz CR, Harwood-Nash DC, Chuang S, et al. Metrizamide ventriculography and computed tomography in infants and children. *Neuroradiology* 1978;16:6–9
14. Yamada H, Nakamura S, Tanaka Y, et al. Ventriculography and cisternography with water-soluble contrast media in infants with myelomeningocele. *Radiology* 1982;143:75–83
15. Naidich TP, Pudlowski RM, Naidich JB. Computed tomographic signs of the Chiari II malformation. I. Skull and dural partitions. *Radiology* 1980;134:65–71
16. Naidich TP, Pudlowski RM, Naidich JB. Computed tomographic signs of the Chiari II malformation: II. Midbrain and cerebellum. *Radiology* 1980;134:391–398
17. Naidich TP, Pudlowski RM, Naidich JB. Computed tomographic signs of the Chiari II malformation: III. Ventricles and cisterns. *Radiology* 1980;134:657–663
18. Naidich TP, McLone DG, Fulling KH. The Chiari II malformation: IV. The hindbrain deformity. *Neuroradiology* 1983;25:179–197
19. Hemmy DC, Millar EA, Houghton V. Gas myelography in the management of spinal cord disorders in children. *Neuroradiology* 1978;16:85–86
20. Hall PV, Campbell RL, Kalsbeck JE. Meningomyelocele and progressive hydromyelia: progressive paresis in myelodysplasia. *J Neurosurg* 1975;43:457–463
21. Zimmerman RD, Breckbill D, Dennis MW, et al. Cranial CT findings in patients with meningomyelocele. *AJR* 1979;132:623–629
22. Yu HC, Deck MDF. The clivus deformity of Arnold-Chiari malformation. *Radiology* 1971;101:613–615
23. El Gammal T, Brooks BS. Radiologic evaluation of the craniovertebral

- junction. In: Taveras JM, Ferrucci JT, eds. *Radiology: diagnosis/imaging/intervention*, vol 3, chapt 70. Philadelphia: Lippincott, **1986**: 1-15
24. Peach B. Cystic prolongation of the fourth ventricle: anomaly associated with the Arnold-Chiari malformation. *Arch Neurol* **1964**;11:609-612
 25. Gooding CA, Carter A, Hoare RD. New ventriculographic aspects of Arnold-Chiari malformation. *Radiology* **1967**;89:626-632
 26. El Gammal T, Allen MB Jr. *An atlas of polytome pneumography*, vol 4. Springfield, IL: Thomas, **1977**:136-138
 27. Sutton D Jr. Radiological assessment of normal aqueduct and 4th ventricle. *Br J Radiol* **1950**;23:208-218
 28. Peach B. Arnold-Chiari malformation with normal spine. *Arch Neurol* **1964**;10:497-501
 29. Swanson HS, Fincher EF. Arnold-Chiari malformation without bony anomalies. *J Neurosurg* **1949**;6:314-319